

See discussions, stats, and author profiles for this publication at: <https://www.researchgate.net/publication/43071870>

Cholesterol Sulfate Imaging in Human Prostate Cancer Tissue by Desorption Electrospray Ionization Mass Spectrometry

ARTICLE *in* ANALYTICAL CHEMISTRY · APRIL 2010

Impact Factor: 5.64 · DOI: 10.1021/ac9029482 · Source: PubMed

CITATIONS

81

READS

25

9 AUTHORS, INCLUDING:



Livia S Eberlin

Stanford University

46 PUBLICATIONS 1,480 CITATIONS

SEE PROFILE



Liang Cheng

Indiana University School of Medicine

818 PUBLICATIONS 17,928 CITATIONS

SEE PROFILE



Michael O Koch

Indiana University School of Medicine

177 PUBLICATIONS 4,426 CITATIONS

SEE PROFILE



Timothy L Ratliff

Purdue University

214 PUBLICATIONS 10,491 CITATIONS

SEE PROFILE

Published in final edited form as:

Anal Chem. 2010 May 1; 82(9): 3430–3434. doi:10.1021/ac9029482.

Cholesterol Sulfate Imaging in Human Prostate Cancer Tissue by Desorption Electrospray Ionization Mass Spectrometry

Livia S. Eberlin¹, Allison L. Dill¹, Anthony B. Costa¹, Demian R. Iff¹, Liang Cheng², Timothy Masterson³, Michael Koch³, Timothy L. Ratliff⁴, and R. Graham Cooks^{1,*}

¹Department of Chemistry and Center for Analytical Instrumentation Development, Purdue University, West Lafayette, IN 47907, USA

²Department of Pathology and Laboratory Medicine, Indiana University School of Medicine, Indianapolis, IN 46202, USA

³Department of Urology, Indiana University School of Medicine, Indianapolis, IN 46202, USA

⁴Purdue University Center for Cancer Research, Purdue University, West Lafayette, IN 47907, USA

Abstract

Development of methods for rapid distinction between cancerous and non-neoplastic tissues is an important goal in disease diagnosis. To this end, desorption electrospray ionization mass spectrometry (DESI-MS) imaging was applied to analyze the lipid profiles of thin tissue sections of 68 samples of human prostate cancer and normal tissue. The disease state of the tissue sections was determined by independent histopathological examination. Cholesterol sulfate was identified as a differentiating compound, found almost exclusively in cancerous tissues including tissue containing precancerous lesions. The presence of cholesterol sulfate in prostate tissues might serve as a tool for prostate cancer diagnosis although confirmation through larger and more diverse cohorts and correlations with clinical outcome data is needed.

Keywords

ambient ionization; prostate cancer; mass spectrometry imaging; tumor marker; biomarker; principal component analysis

Evidence is provided that cholesterol sulfate might serve as an indicator for prostate cancer, following its detection by desorption electrospray ionization (DESI) imaging mass spectrometry (MS) in prostate tissue samples shown by histopathological examination to be cancerous or precancerous. The desire to distinguish rapidly between diseased and healthy tissues (even *in vivo* or intra-operatively) makes it important to identify new molecular targets for disease detection and diagnosis. As part of a program aimed at addressing these issues, DESI-MS imaging was applied to analyze the lipid profiles of thin tissue sections of human prostate cancer under ambient conditions and to compare these images with those for non-cancerous tissue, typed as normal tissue in routine histopathological examination. Cholesterol sulfate (CS) was observed almost exclusively in cancerous tissues and high grade prostatic intraepithelial (PIN) neoplasia as determined by histopathological examination, but it was not

*Corresponding Author Professor R. Graham Cooks, Department of Chemistry, Purdue University, West Lafayette, IN, 47907, Tel: (765) 494-5262, Fax: (765) 494-9421, cooks@purdue.edu.

Supporting Information

Additional information as noted on text.

detected in normal tissue by DESI-MS. This is the first report of CS as a potential tumor marker for human prostate cancer.

Mass spectrometry has long been used to image the distributions of proteins, lipids and other specific compounds in tissue. This information is potentially valuable in the development of new disease diagnostic methods and in advancing the fundamentals of disease biology.²⁻⁴ Amongst the MS imaging methods, DESI-MS allows ambient tissue imaging^{5, 6} and it appears from preliminary studies to have significance in disease diagnosis in several organs, including provision of information on tumor margins from the spatial distributions of phospholipids.⁷ Correlations between the spatial distributions of a broad range of biomolecules in tissue samples provide information that could be important in the diagnosis and treatment of disease.⁸ The abundance of ions of any particular m/z value and hence the distribution of the corresponding molecule in the tissue sample can be represented in the form of a DESI-MS image. Although the methodology can be used to generate an image of any ion observed in the mass spectrum, selected ion images from limited set of molecular species for each sample analyzed are most useful and these are displayed here.

Amongst the most abundant signals detected in the negative ion DESI mass spectrum of tissue samples are those due to fatty acids and polar lipids. It is known that alterations in the lipid composition of tissues occur in various forms of cancer.^{9, 10} In particular, cholesterol sulfate (CS), an important sterol sulfate present in a variety of mammalian tissues and known for its stabilizing and regulatory role as a cell membrane component, has been reported¹¹ as a potential tumor marker in human uterine cervical carcinoma tissue. The same study showed that CS is co-expressed with transglutaminase-1 and cytokeratin in well-differentiated types of squamous cell cancers as a tumor marker. Increased accumulation of CS has also been observed in tumorigenic esophageal rat cells.¹²

DESI-MS imaging data on human prostate tissue presented here show that CS is found almost exclusively in cancerous tissues and high grade prostatic intraepithelial neoplasia (PIN), a pathology considered to represent precancerous lesions. These correlations are based on standard histological hematoxylin and eosin (H&E) stained sections and DESI-MS acquired images. This behavior of CS is qualitatively different to that of other lipids, including particular glycerophospholipids (GPs) and free fatty acids (FAs) which occur in both diseased and healthy tissue samples although with differences in relative amounts.

Mass spectra and ion images from the analysis of 68 prostate tissue samples from 34 different patients were obtained by DESI-MS. Identification of the compounds responsible for the peaks observed in the mass spectra was made based on collision-induced dissociation (CID) tandem MS experiments and by comparison of the product-ion mass spectra to reported literature data or to spectra generated from the standard compounds.¹³ The ions observed correspond to three major lipid classes; glycerophosphoinositols (PI), glycerophosphoserines (PS) and fatty acids (FA). A peak at mass/charge ratio (m/z) 465.4 was observed at high relative abundance during the analysis of cancerous prostatic tissues (Figure 1A) and was not detected in normal tissue (Figure 1B). This peak was tentatively assigned as cholesterol sulfate and when these ions were subjected to tandem MS experiments for structure elucidation, the main fragment ion was observed at m/z 97.0 and assigned as the $[\text{HSO}_4]^-$ ion (Figure 1C). The standard compound, sodium cholesteryl sulfate (Sigma-Aldrich Inc., Milwaukee, WI), was subjected to tandem MS experiments under the same conditions and gave identical results (Figure 1D). For further confirmation, the isotopic distribution of the molecular ion at m/z 465.4 (insets of Figures 1C and 1D) was found to agree with the proposed molecular formula.¹⁴

The association of cholesterol sulfate, identified by the DESI-MS data, with diseased tissue is provided by pathological examination of the H&E stained sections. The latter information is

used to label the tissue sections in the figures shown below. All human tissue samples were handled in accordance with approved institutional review board (IRB) protocols at Indiana University School of Medicine. Standard DESI-MS imaging conditions were used to analyze the tissue samples in the negative ion mode (Materials and methods are available in the Supporting Information). In addition to displaying cholesterol sulfate images from individual tissue sections, principal component analysis (PCA) was employed to generate images of these sections from the entire set of DESI mass spectra. The resulting PCA images represent a simple and unsupervised way to visually inspect all the DESI data for identification of tumor and normal regions based on color-coded differences between the tumor and normal samples. Further analysis of the PCA-derived loading plots shows the peak corresponding to cholesterol sulfate to be a primary contribution to separation of tumor and control in the generated images (Figure S1, Supporting Information), reinforcing the conclusions of this work. Since diagnosis in this case, based on the detection of cholesterol sulfate, is so clear-cut no advantage is gained by extending the data analysis to other compounds.

Representative tumor and normal tissue section images from one patient, case number MH0107-01, are shown in Figure 2 (tumor and normal tissue appear on the left and right side of the images, respectively). Similar intensities were observed for m/z 788.4 (PS(18:0/18:1)) (Figure 2A) and m/z 885.5 (PI(18:0/20:4)) (Figure 2B). The notation (X:Y) represents the number of carbon atoms and double bonds in the fatty acid chains, respectively. Remarkably, cholesterol sulfate (m/z 465.4) was observed exclusively in the cancerous tissue, enabling its clear identification (Figure 2C). To broaden the analysis, the diagnosis was supported by the PCA generated image which also reveals clear differences between the tumor and normal tissues (Figure S3). Cancerous and normal prostate tissue samples from another patient, case number MH0301-17 (Figure S4) show the same relative intensity in disease and normal tissue for the selected PS, PI and FA ions. The cancerous tissue is most clearly identified by observing the significantly increased intensity of CS which is undetectable in the normal tissue.

H&E stained and DESI-MS images of CS are shown for another 10 tissue samples in Figure 3. For the samples shown in panels A, B and C, CS signals are observed in certain regions of the otherwise normal tissue in the DESI ion images, which correspond to precancerous lesions or high grade prostatic intraepithelial neoplasia (PIN) as determined by pathological examination. The sample shown Figure 3D consists of another case in which one tissue section is completely normal and the other has PIN, and where CS is undetectable in the normal tissue and present in regions of the PIN section. Figure 3E shows a case in which both tissue sections contain PIN, with corresponding CS by DESI-MS. High grade PIN is characterized by a proliferation of malignant prostatic epithelial cells in prostatic ducts and acini and it is a precursor to the majority of prostatic adenocarcinomas.

A close examination of the image obtained for CS shown in Figure 2C, reveals that within the normal tissue, a small localized signal for CS was observed at a spot near the bottom of the tissue. This indicated that a region of PIN might be present in the normal tissue section and in order to follow up on this indication, twenty additional serial sections for this tissue specimen (case number MH0107-01) comprising the entire tissue were analyzed. Ten serial sections spaced throughout the 20 sections used for DESI-MS analysis were subjected to independent H&E staining. Pathological examination of these additional H&E stained tissue sections as well as the original H&E stained section (Figure 2D) confirmed that the specific region in which CS is observed contains precancerous lesions, or high grade prostatic intraepithelial neoplasia (PIN). Ion images of CS for four of these sections are shown in Figure 2 (E-H) and the additional sixteen sections are shown in Figure S2. In all the tissue sections analyzed, CS signal was undetectable in the normal tissue region while it was observed as the main peak in mass spectra recorded for the cancerous tissue as well as in the small region of the normal tissue identified as containing PIN.

In addition to the above 20 sections from a single patient, a total of 68 tissue samples from 34 different patients were analyzed by DESI-MS imaging. Of the 68 tissue samples, 7 were diagnosed following H&E staining as normal tissue, 19 as cancerous tissue, 30 as containing PIN within normal tissue, 4 as containing cancer cells and PIN and 8 as probable PIN, as described in detail in Table S1. Cholesterol sulfate detection by DESI-MS correctly correlated to cancerous or high grade PIN tissue as determined from pathological examination of the H&E stained tissues in 64 of the 68 tissue samples. In addition to the results already shown, those for some additional samples are displayed in Figures S5 and S6 in the Supporting Information. In two of the four non-correlating samples, cholesterol sulfate was detected in localized regions within the normal tissues, potentially indicating the presence of precancerous lesions, but pathological examination of the H&E stained sections did not confirm this (results for one of these two samples are presented in Figure S7 in the Supporting Information). Two interpretations are possible, first that these two cases are false positives and second, the results obtained for these two samples indicate early stage prostatic neoplasia not yet discernible by morphological examination. The other two non-correlating tissue samples are from a sample pair which yielded completely inverted results; CS was detected in normal tissue and not detected in cancerous tissue, resulting in both a false positive and a false negative. Overall, the results suggest that DESI tissue imaging not only enables clear differentiation between cancerous and normal tissues due to the presence of the tumor marker CS but that it might also be useful to detect precancerous lesions found within normal tissues. This preliminary interpretation is made with caution, especially given continuing concerns regarding unsubstantiated claims of biomarkers.¹⁵ The presence of cholesterol sulfate in prostate tissues might serve as a tool for prostate cancer diagnosis although confirmation through larger and more diverse cohorts and correlations with clinical outcome data are needed.

Future studies will also focus on investigating and understanding the biological processes responsible for the differential expression of CS in human prostate cancer and its role in malignancy. The metabolic state associated with high levels of CS in prostate cancer is not known but it could be linked to known high fatty acid synthesis and/or androgen synthesis^{16–18}. Furthermore, CS is known to be an activator of the η isoform of protein kinase C (PKC), which is expressed in epithelial tissues and involved in cellular differentiation, indicating that CS modifies cell carcinogenesis.¹⁹ CS also regulates serine proteases perhaps including prostate-specific antigen (PSA), the main biomarker currently used in screening for prostate cancer in human serum. Therefore, it is possible that the metastatic activity that affects PSA levels directly or indirectly affects CS levels. We expect that CS should be detectable at increased levels in the biological fluids of prostate cancer patients. If so, correlations should be sought between these levels and independent makers of disease progression in an attempt to provide a tool for improved disease management.

Supplementary Material

Refer to Web version on PubMed Central for supplementary material.

Acknowledgments

Financial support was provided by the U.S. National Institutes of Health (Grant 1R21EB009459-01). The authors thank Dr. Scott Crist for valuable discussions.

References

1. Schafer KC, Denes J, Albrecht K, Szaniszlo T, Balog J, Skoumal R, Katona M, Toth M, Balogh L, Takats Z. *Angew. Chem. Int. Edit* 2009;48:8240–8242.
2. MacAleese L, Stauber J, Heeren RM. *A. Proteomics* 2009;9:819–834.

3. Seeley EH, Caprioli RM. *Proteom. Clin. Appl* 2008;2:1435–1443.
4. Walch A, Rauser S, Deininger SO, Hofler H. *Histochem. Cell Biol* 2008;130:421–434. [PubMed: 18618129]
5. Kertesz V, Van Berkel GJ, Vavrek M, Koeplinger KA, Schneider BB, Covey TR. *Anal. Chem* 2008;80:5168–5177. [PubMed: 18481874]
6. Wiseman JM, Ifa DR, Venter A, Cooks RG. *Nat. Protoc* 2008;3:517–524. [PubMed: 18323820]
7. Dill AL, Ifa DR, Manicke NE, Costa AB, Vara JAR, Knapp DW, Cooks RG. *Anal. Chem* 2009;81:8758–8764. [PubMed: 19810710]
8. Hardesty WM, Caprioli RM. *Anal. Bioanal. Chem* 2008;391:899–903. [PubMed: 18365184]
9. Glunde K, Jie C, Bhujwalla ZM. *Cancer Res* 2004;64:4270–4276. [PubMed: 15205341]
10. Iorio E, Mezzanzanica D, Alberti P, Spadaro F, Ramoni C, D'Ascenzo S, Millimaggi D, Pavan A, Dolo V, Canevari S, Podo F. *Cancer Res* 2005;65:9369–9376. [PubMed: 16230400]
11. Kiguchi K, Iwamori M, Yamanouchi S, Ishiwata L, Saga M, Amemiya A. *Clin. Cancer Res* 1998;4:2985–2990. [PubMed: 9865910]
12. Rearick JI, Stoner GD, George MA, Jetten AM. *Cancer Res* 1988;48:5289–5295. [PubMed: 3409253]
13. Pulfer M, Murphy RC. *Mass Spectrom. Rev* 2003;22:332–364. [PubMed: 12949918]
14. Metzger K, Rehberger PA, Erben G, Lehmann WD. *Anal. Chem* 1995;67:4178–4183.
15. Hughes V. *Nat. Med* 2009;15:1339–1343. [PubMed: 19966757]
16. Migita T, Ruiz S, Fornari A, Fiorentino M, Priolo C, Zadra G, Inazuka F, Grisanzio C, Palescandolo E, Shin E, Fiore C, Xie W, Kung AL, Febbo PG, Subramanian A, Mucci L, Ma J, Signoretti S, Stampfer M, Hahn WC, Finn S, Loda M. *J. Natl. Cancer Inst* 2009;101:519–532. [PubMed: 19318631]
17. Titus MA, Schell MJ, Lih FB, Tomer KB, Mohler JL. *Clin. Cancer Res* 2005;11:4653–4657. [PubMed: 16000557]
18. Williams ML, Rutherford SL, Feingold KR. *J. Lipid. Res* 1987;28:955–967. [PubMed: 2444666]
19. Kuroki T, Ikuta T, Kashiwagi M, Kawabe S, Ohba M, Huh N, Mizuno K, Ohno S, Yamada E, Chida K. *Mutat. Res. Rev. Mutat. Res* 2000;462:189–195.

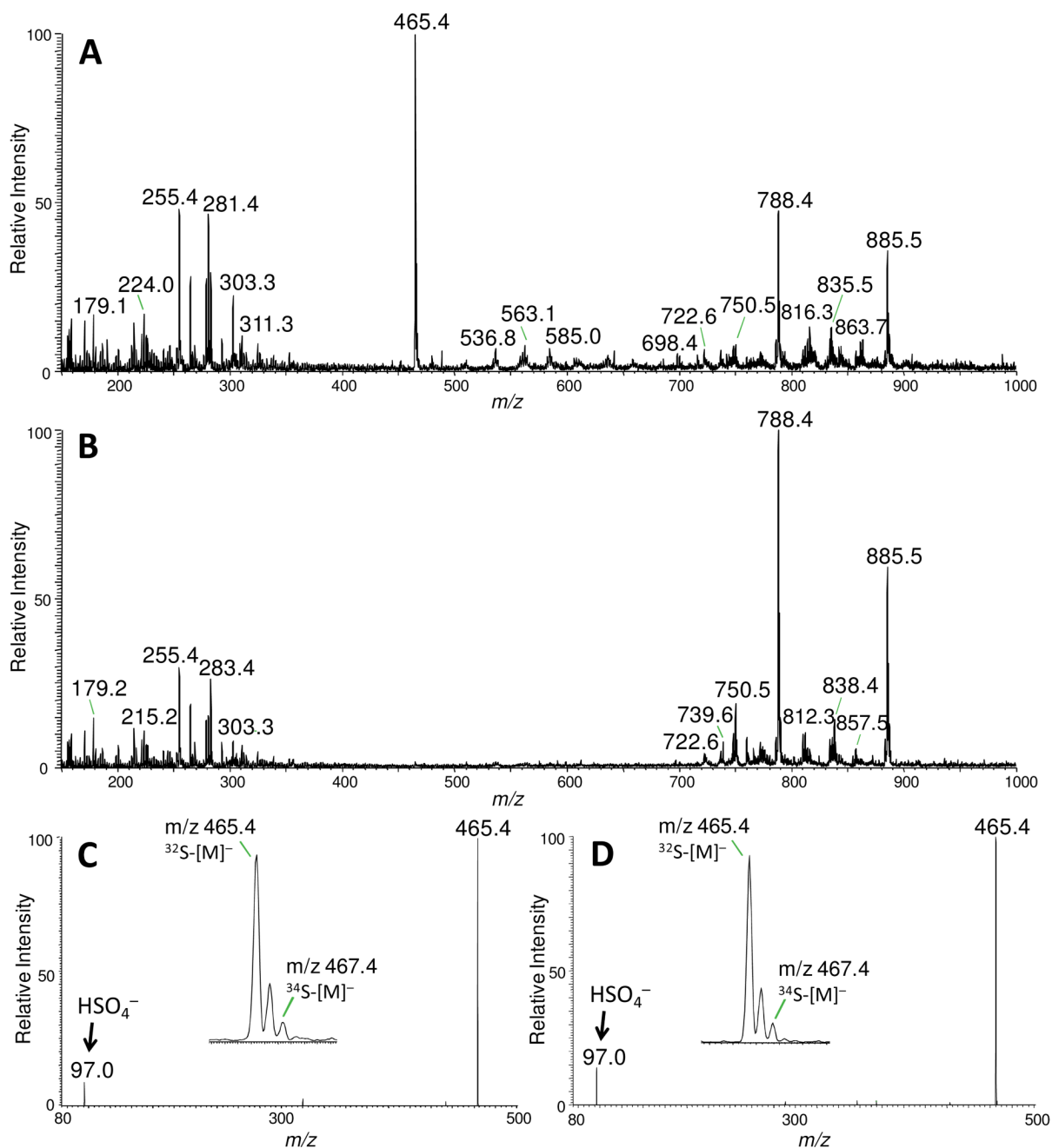
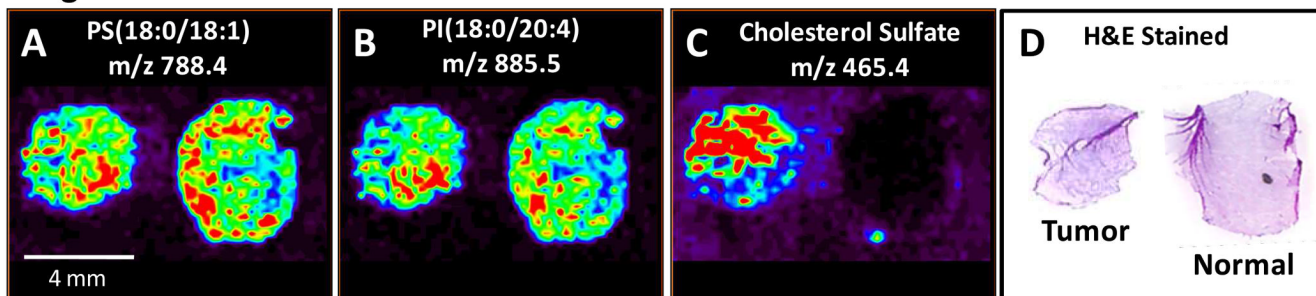
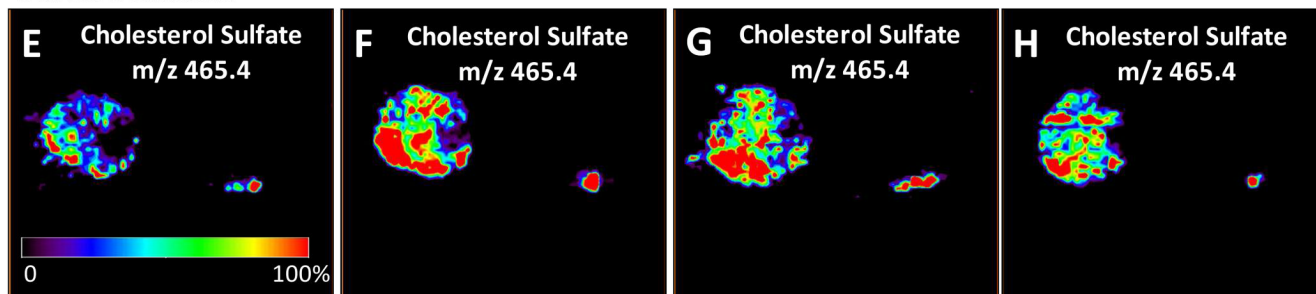


Figure 1.

Typical negative ion mode mass spectra of (A) human prostate cancer and (B) normal tissue in the range of m/z 150 – 1000. Tandem mass spectra (C) of assigned cholesterol sulfate (m/z 465.4) from human prostate cancer tissue and (D) of standard cholesterol sulfate sample. The insets show the isotopic patterns of respective cholesterol sulfate ions. The characteristic fragment ion at m/z 97 was observed for both the standard and the molecule detected in prostatic tissue.

Original Section**Serial Sections****Figure 2.**

Negative ion mode tissue imaging of prostate tissue showing areas of cancer and normal tissue in sample MH0107-01 (left and right sides, respectively, for each of eight images). (A) Ion image of m/z 788.4, PS(18:0/18:1), (B) Ion image of m/z 885.5, PI(18:0/20:4), (C) Ion image of m/z 465.4, cholesterol sulfate and (D) H&E stained tissue sections of the tumor tissue and normal. Ion images of m/z 465.4, cholesterol sulfate, in four additional sections taken from among 135 serial sections obtained by cutting a 2.7 mm thick tissue block into serial sections are shown as E-H.

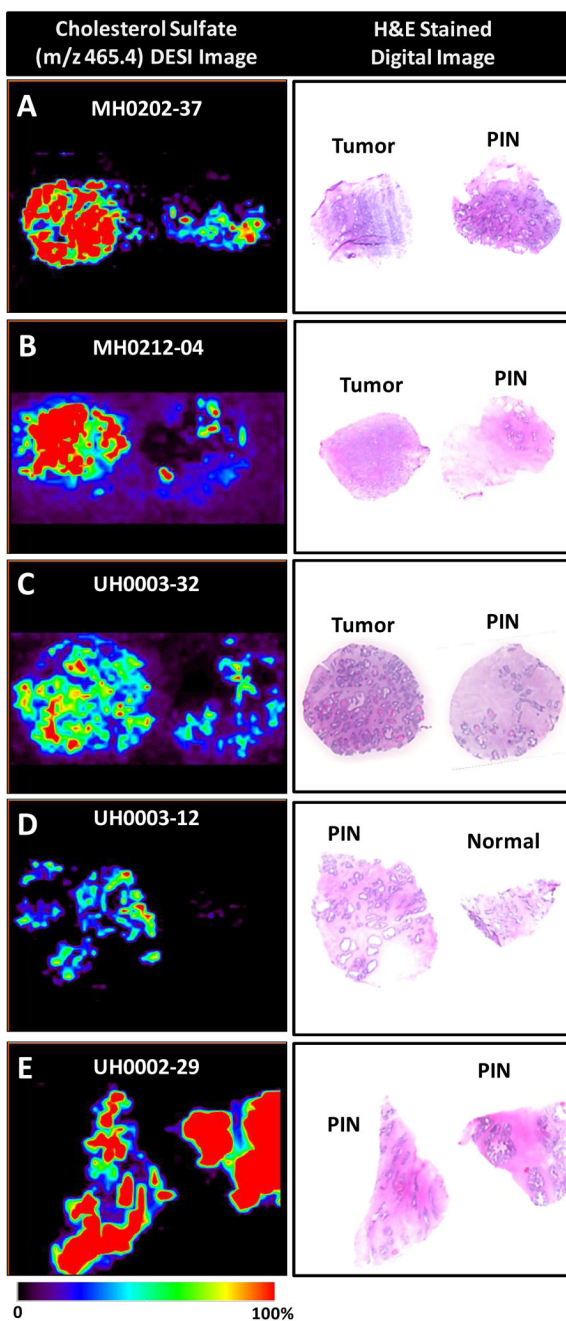


Figure 3.

DESI-MS ion image of m/z 465.4, cholesterol sulfate, in the negative ion mode, and H&E stained image of prostate samples (A) MH0202-37, cancer and adjacent normal tissue with PIN, (B) MH212-04, cancer and normal tissue with PIN, (C) UH0003-32, cancer and normal tissue with PIN, (D) UH0003-12, PIN and normal tissue and (E) UH0002-29, PIN detected within normal regions of tissue.